Korean J. Chem. Eng., **25**(6), 1546-1552 (2008)

Hydrothermal synthesis of zeolite L in a Na^+/K^+ mixed alkali system

Yong Sig Ko* and Wha Seung Ahn,†**

*Department of Advanced Material Chemistry, Shinsung University, Dangjin-gun 343-860, Korea
**School of Chemical Science and Engineering, Inha University, Incheon 402-751, Korea
(*Received 13 February 2008 • accepted 29 March 2008*)

Abstract−Zeolite L was prepared from the substrate system of Na_2O-K_2O-Al_2O_3-SiO_2-H_2O at temperatures of 373-443 K by hydrothermal crystallization. The influence of various synthesis parameters such as the concentration ratios of the components, starting raw materials, synthesis temperature, gel aging, and stirring on the crystallization was investigated. Investigations revealed that the crystallinity of zeolite L crystals depends on molar ratios of the components such as SiO_2/Al_2O_3, $(K_2O+Na_2O)/SiO_2$, $Na_2O/(K_2O+Na_2O)$, and $H_2O/(K_2O+Na_2O)$. Pure and highly crystalline zeolite L could be obtained from a gel with the molar composition $5.4K_2O$-$5.7Na_2O$-Al_2O_3-$30SiO_2$-$500H_2O$ after 24 h at 443 K. It was found that the silica source affected the crystal size of zeolite L, and as the synthesis temperature increased, the average crystal size became larger. The crystal size could be decreased significantly by stirring the gel or subjecting the substrate mixture to an aging treatment at room temperature prior to the hydrothermal treatment. Thermal stability of the zeolite L crystals obtained was also briefly investigated.

Key words: Zeolite L, Hydrothermal Synthesis, Aging, Morphology, Thermal Stability

INTRODUCTION

Zeolite L is a crystalline aluminosilicate molecular sieve featuring a hexagonal symmetry [1]. It possesses one-dimensional pore of about 0.71 nm aperture leading to cavities of about 0.48×1.24 1.07 nm, and the framework of the Si/Al ratio is typically about 3.0 [1,2]. By virtue of its unique structure and composition, zeolite L has attracted great research interest in its synthesis and characterization [3-6], adsorptive properties [7-9], mixed matrix membranes [10-13] and catalytic application in various hydrocarbon conversion reactions [14-22]. Pt supported on alkaline zeolites is best known as a remarkable catalyst for the aromatization of alkanes [14-19]. It was reported that the interesting performance of Pt/zeolite L is owing to a collimating (geometric) effect [21], and the zeolite L can thus stabilize very small Pt clusters [17]. More recently, Calzaferri and coworkers [23-26] have also shown that zeolite L is a convenient host for the supramolecular organization of dyes. Recently, Joshi et al. [3] reported the influence of various synthesis variables on crystallization kinetics, product composition, morphology and yield of zeolite KL from K_2O-Al_2O_3-SiO_2-H_2O system. Yoon et al. [6] synthesized a flat faceted zeolite L with a length longer than 15 μm. Although a considerable amount of information is available on the preparation of zeolite L, more detailed investigation on the effect of synthesis conditions in a Na^+/K^+ mixed alkali system on crystal morphology is desired.

In this study, we extended our earlier work [27,28] on hydrothermal synthesis of zeolite L in the synthesis system of K_2O-Na_2O-Al_2O_3-SiO_2-H_2O system to emphasize the morphological details of the crystals obtained. Efforts were primarily given to verify the optimum substrate composition to obtain high-purity zeolite L crystals with small and uniform particle size.

EXPERIMENTAL

1. Hydrothermal Synthesis of Zeolite L

In preparing the substrates for hydrothermal synthesis, the sources used for silica were colloidal silica sol (Ludox HS-40 from Dupont,

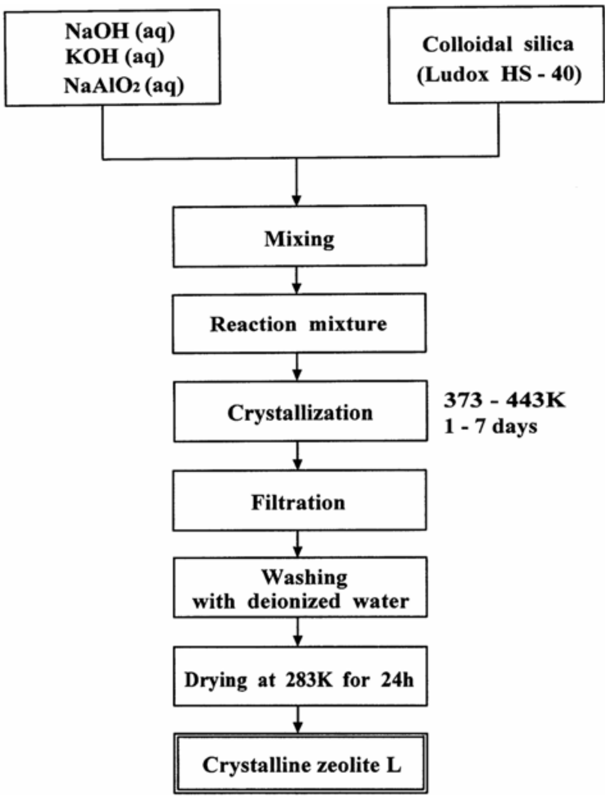

Fig. 1. Schematic diagram for the hydrothermal synthesis of zeolite L.

[†] To whom correspondence should be addressed.
E-mail: whasahn@inha.ac.kr

40% SiO_2), fine silica powder of Zeosil 77 (KoFran Co., 91.8% SiO_2), aqueous sodium silicate solution (KoFran Co., 25.3% SiO_2, 6.6% Na_2O). Sodium aluminate (Junsei Co., 32.6% Na_2O, 35.7% Al_2O_3), aluminum hydroxide (Junsei Co., 51.1% Al_2O_3) and aluminum sulfate (Shinyo Co., 56% Al_2O_3) were used as sources of alumina. Potassium hydroxide (Tedia Co., 85%) and sodium hydroxide (Tedia Co., 98%) were used for alkali metal cations.

Zeolite L was prepared from substrates having the following composition range expressed as oxide mole ratios: SiO_2/Al_2O_3=10-35, $(K_2O+Na_2O)/SiO_2$=0.30-0.55, $Na_2O/(K_2O+Na_2O)$=0.20-0.68, $H_2O/(K_2O+Na_2O)$=30-60. The substrates for the synthesis of zeolite L were typically prepared according to the procedure published in Ref. [28]. The synthesis procedure of zeolite L described above is schematically represented in Fig. 1.

2. Characterization

The samples prepared were analyzed by X-ray diffraction (XRD) for phase identification. The unit used was a powder X-ray diffractometer (Philips, PW-1700) with a scintillation counter and a graphite monochromator attachment, utilizing Ni-filtered CuKα radiation. To calculate crystallinity, peaks located at 2θ=5.5, 19.4, 22.7, 28.0, 29.1 and 30.7 were used to avoid the possible interference of the coexisting phases for a given sample. A pure sample with the most intense peaks was taken as reference assigning 100% crystallinity, and the percentage crystallinity of the other samples was calculated relative to the reference. The morphology of the crystalline phase was examined by using a scanning electron microscope (SEM, Hitachi, X-650) after coating with an Au-Pd evaporated film.

RESULTS AND DISCUSSION

Fig. 2 shows the typical X-ray diffraction pattern of the zeolite L sample obtained in 24 h at 443 K for a given set of synthesis conditions. Characteristic XRD peaks show that highly crystalline zeolite L crystals were obtained and the XRD pattern closely agrees with the literature [29,30].

Zeolite L was prepared from a substrate composition of $5.4K_2O$-$5.7Na_2O$-Al_2O_3-$30SiO_2$-$500H_2O$ at different synthesis temperatures of 373-443 K. SEM photographs of the zeolite L crystals obtained with different synthesis temperatures under the same crystallization conditions are shown in Fig. 3. With the increasing synthesis temperature, the crystal size of zeolite L gradually became larger; both the rate of nucleation and crystal growth at high temperature are

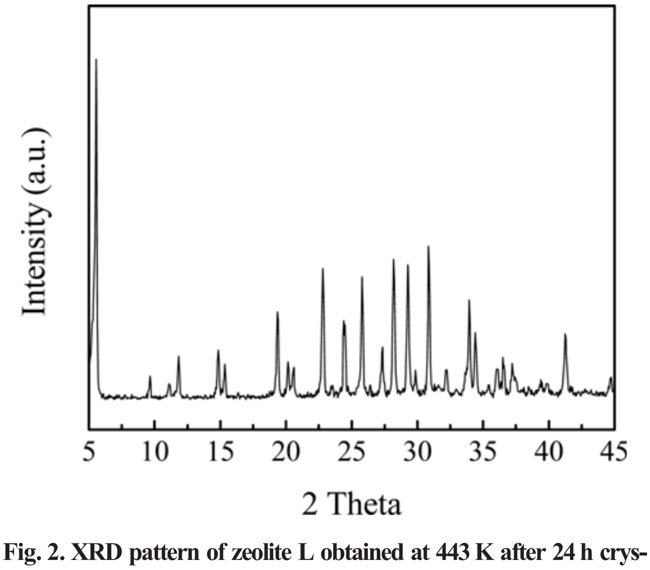

Fig. 2. XRD pattern of zeolite L obtained at 443 K after 24 h crystallization.

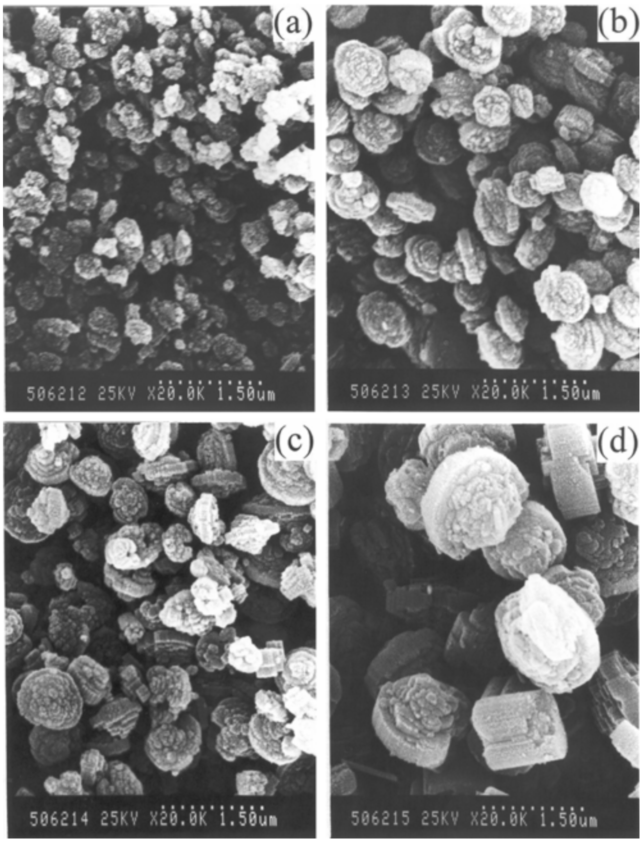

Fig. 3. SEM photographs of zeolite L crystals synthesized at different reaction temperatures. (a) 373 K, (b) 403 K, (c) 423 K, and (d) 443 K.

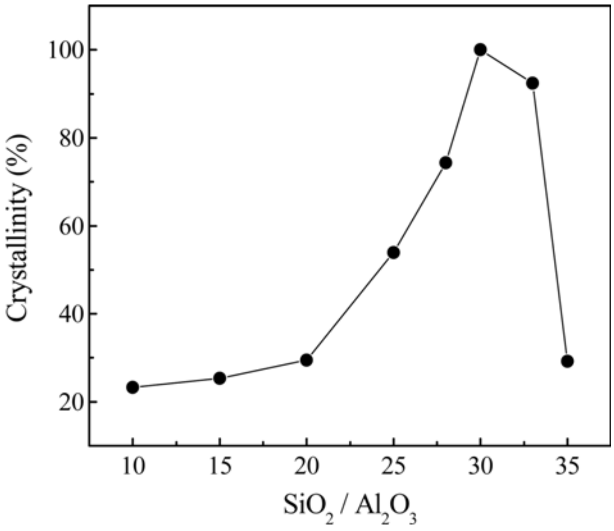

Fig. 4. Effect of SiO_2/Al_2O_3 ratio on zeolite L crystallization at 443 K. $(K_2O+Na_2O)/SiO_2$=0.37, $H_2O/(K_2O+Na_2O)$=45, $Na_2O/(K_2O+Na_2O)$=0.5, 24 hr synthesis.

much faster than those at lower temperature.

Initial composition of any substrate mixture is very important in determining the zeolite types to be formed, and especially, the SiO_2/Al_2O_3 ratio is a critical factor for the zeolite phase obtained and its yields [31]. Fig. 4 shows the effect of SiO_2/Al_2O_3 ratios of the synthesis mixture on the zeolite L crystallization at constant $(K_2O+Na_2O)/SiO_2$, $Na_2O/(K_2O+Na_2O)$ and $H_2O/(K_2O+Na_2O)$ ratios. The crystallinity for the zeolite L increased substantially with an increase in the SiO_2/Al_2O_3 ratio in the range of 20 to 30. With increasing SiO_2/Al_2O_3 ratio in the synthesis mixture, the crystallization rate is also increased, which is a common observation made in the synthesis of high silica molecular sieves [3,32-35]. This phenomenon can be interpreted with an increasing viscosity of the gel which results in a faster rate of nucleation. It was found that zeolite L could be obtained as a pure phase and with good crystallinity at the SiO_2/Al_2O_3 ratio around 30. While at a SiO_2/Al_2O_3 ratio higher than 30, the crystallinity decreased. If the SiO_2/Al_2O_3 ratio is too high or low, the system forms zeolite T or W, respectively, which appear to be the thermodynamically more stable phases.

The change in alkali concentration in the synthesis mixture may cause a change in the rate of nucleation, and so does the presence of hydroxide ions which strongly affects the formation of nuclei. When solutions of the aluminate and silicate or polysilicate anions are mixed to form the hydrogels, a strong base such as NaOH or KOH accelerates the dissolution of the gel materials and the formation of $Al(OH)_n$. The dissolved silicate and aluminate ions can also undergo a polymerization process to aluminosilicate or polysilicate ions. The soluble aluminosilicate or polysilicate species may subsequently regroup around the hydrated anion to form the nuclei of the ordered zeolite. There exists a quasi-equilibrium between the dissolved species, the gel and the nuclei formed in the liquid phase.

Fig. 5 shows the effect of $(K_2O+Na_2O)/SiO_2$ ratios of the synthesis mixture on the zeolite L crystallization at constant SiO_2/Al_2O_3, $Na_2O/(K_2O+Na_2O)$ and $H_2O/(K_2O+Na_2O)$ ratios. It can be seen that crystallization for the zeolite L strongly depends on $(K_2O+Na_2O)/SiO_2$ ratios. In the range of $(K_2O+Na_2O)/SiO_2$ ratios lower than 0.37, the increase of $(K_2O+Na_2O)/SiO_2$ led to a gradual increase in the content of zeolite L phase. It seems that the increase of alkalinity effectively induced the dissolution of the amorphous aluminosilicate gel in the reaction mixture to form soluble active species, and crystallization rate has been increased with increasing $(K_2O+Na_2O)/SiO_2$ ratio [3]. However, at higher $(K_2O+Na_2O)/SiO_2$ ratios above 0.37, the degree of crystallization for the zeolite L decreased again as the ratios increased. This indicates that the polycondensation of hydroxoaluminate and silicate species is restricted by excess alkalinity [3]. Thus, an increase in alkalinity can cause a decrease in the induction period and shorten the overall crystallization period, but higher alkalinity beyond a threshold value may prolong the nucleation time. These results suggest the existence of an optimum alkalinity for nucleation in the synthesis of zeolite L. Results obtained from these series of experiments show that the optimum ratio of the $(K_2O+Na_2O)/SiO_2$ is around 0.37 when varying the $(K_2O+Na_2O)/SiO_2$ ratio from 0.30 to 0.55.

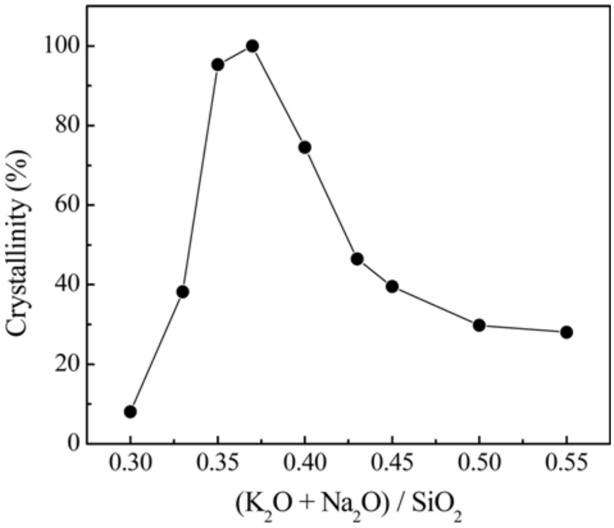

Fig. 5. Effect of $(K_2O+Na_2O)/SiO_2$ ratio on zeolite L crystallization at 443 K. SiO_2/Al_2O_3=30, $H_2O/(K_2O+Na_2O)$=45, $Na_2O/(K_2O+Na_2O)$=0.5, 24 h synthesis.

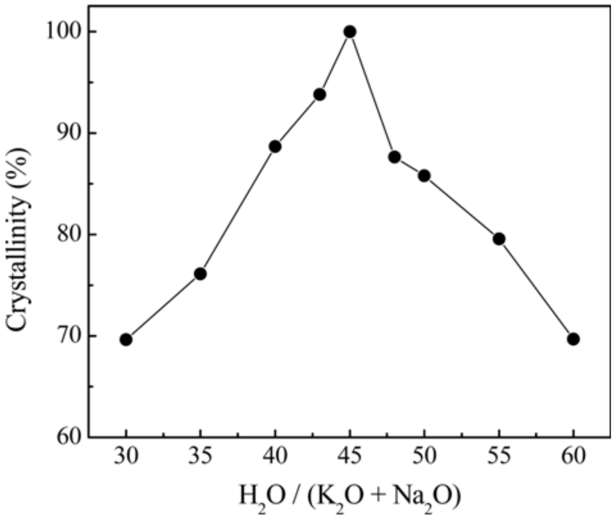

Fig. 6. Effect of $H_2O/(K_2O+Na_2O)$ ratio on zeolite L crystallization at 443 K. SiO_2/Al_2O_3=30, $(K_2O+Na_2O)/SiO_2$=0.37, $Na_2O/(K_2O+Na_2O)$=0.5, 24 h synthesis.

Fig. 6 shows the effect of $H_2O/(K_2O+Na_2O)$ ratios of synthesis mixture on the zeolite L crystallization at constant SiO_2/Al_2O_3, $(K_2O+Na_2O)/SiO_2$ and $Na_2O/(K_2O+Na_2O)$ ratios. It was shown that the water content in the synthesis mixture also played an important role in the synthesis of zeolite L. The degree of crystallinity for the zeolite L increased remarkably as the $H_2O/(K_2O+Na_2O)$ ratio increased from 30 up to around 45. In fact, the ratio of $H_2O/(K_2O+Na_2O)$ determines the concentration of the gel if the other three ratios are kept constant, and the viscosity of the synthesis gel changes with changing water content. Therefore, it may influence the rates of nucleation and crystallization. However, the phenomenon can also be explained as a consequence of the alkalinity variation, rather than the overall changes in gel concentration. The $H_2O/(K_2O+Na_2O)$ ratio in the synthesis mixture represents the inverse of the alkalinity. As seen in the figure, pure zeolite L was formed at the $H_2O/(K_2O+Na_2O)$ ratio of around 45.

Influence of the replacement of K^+ by Na^+ and vice versa on the crystallization kinetics, crystalline phase purity and crystal mor-

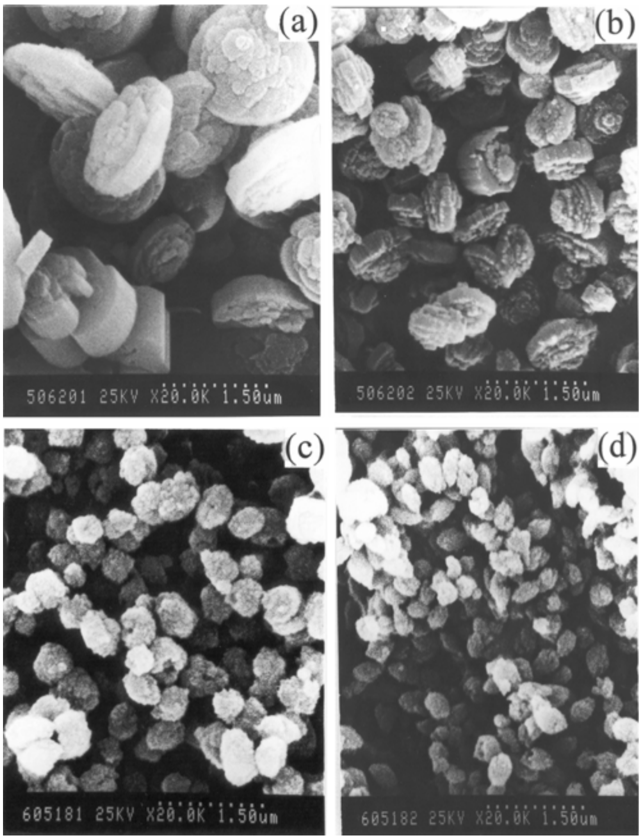

Fig. 7. SEM photographs of zeolite L crystals obtained with different $Na_2O/(K_2O+Na_2O)$ ratios in the synthesis mixture. (a) 0.45, (b) 0.5, (c) 0.55, and (d) 0.6.

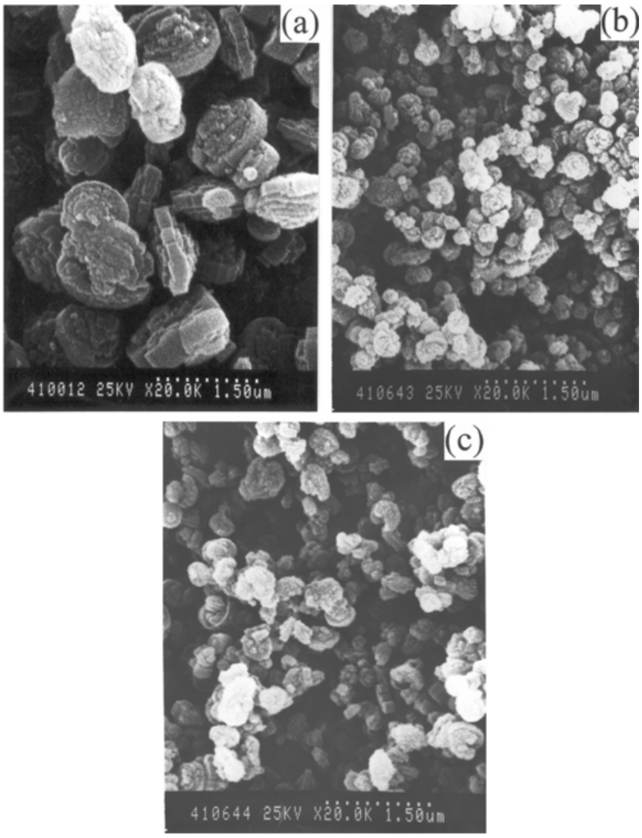

Fig. 8. SEM photographs of zeolite L crystals obtained with different silica sources. (a) Ludox HS-40, (b) Zeosil, and (c) Na_2SiO_3+Zeosil.

phology has been reported [6,28]. Sodium replacement of potassium ions, which is given by the $Na_2O/(K_2O+Na_2O)$ ratio in the reaction mixture, was found to affect the degree of crystallinity for the zeolite L [27]. Pure zeolite L could be obtained in highly purity at the optimum $Na_2O/(K_2O+Na_2O)$ ratio of around 0.5.

Fig. 7 shows the SEM photographs of the zeolite L samples with various $Na_2O/(K_2O+Na_2O)$ ratios at constant SiO_2/Al_2O_3, $(K_2O+Na_2O)/SiO_2$ and $H_2O/(K_2O+Na_2O)$ ratios. The SEM photographs of the final products obtained in this experiment illustrate that the crystal shape was independent of the ratio of $Na_2O/(K_2O+Na_2O)$ in the synthesis gel. Regardless of the ratio, all of the zeolite L samples synthesized showed the clam-shaped crystals. For the batches in which the Na^+ replacement of K^+ was less than 60%, increasing the ratio of $Na_2O/(K_2O+Na_2O)$ led to an increase of the number of nuclei, resulting in zeolite crystals of a smaller average size.

The nature of silica and alumina sources has a great influence on the morphology of the produced zeolite crystals [36,37]. The zeolite L samples were obtained with different silica sources. Three silica sources, viz., colloidal silica sol (Ludox HS-40), amorphous fine silica powder (Zeosil) and sodium silicate solution in conjunction with Zeosil, were tried. Fig. 8 shows the morphology of zeolite L crystals obtained from different silica sources. Typical clam-shaped zeolite L crystals were obtained in this system. Simultaneously, in the cases of using the Zeosil or sodium silicate solution in conjunction with Zeosil as silica source, crystal sizes were smaller than that produced by using Ludox HS-40. The zeolite L samples obtained with Ludox HS-40, Zeosil, and sodium silicate solution in conjunction with Zeosil had average crystal sizes of 1.46, 0.39 and 0.41 μm, respectively.

The zeolite L samples were prepared from the gel aged for 1 day with Ludox and Zeosil as silica source. Fig. 9 shows the morphology of zeolite L crystals obtained from the gel aged for 1 day by using Ludox and Zeosil as silica source under static conditions. For both of the silica sources, aging of the initial gel prior to crystallization also led to a decrease in the average crystal size of zeolite L. Numerous studies have been conducted in which the synthesis gel was aged at low temperature prior to crystallizing at elevated temperatures [38-40]. It is believed that the aging treatment offers the time required to achieve the formation of nuclei with dissolution of silica sources.

Usually, stirring a gel during crystallization results in a decrease in the size of the zeolite particles. However, stirring can also change the zeolite structure [41]. Fig. 10 shows the effect of stirring of the synthesis gel on the zeolite L crystallization. Stirring of the synthesis mixture during the hydrothermal reaction produced a significant increase in crystallization rate of zeolite L. Along with the stirring of synthesis gel, the rates of nucleation and crystallization increased. No other crystalline phases were detected in the XRD patterns of these samples. Fig. 11 shows the morphology of zeolite L crystals prepared under stirring or static condition. SEM photographs show that stirring the gel during crystallization strongly decreased the crystal size of zeolite L and the sample was in the form of very small

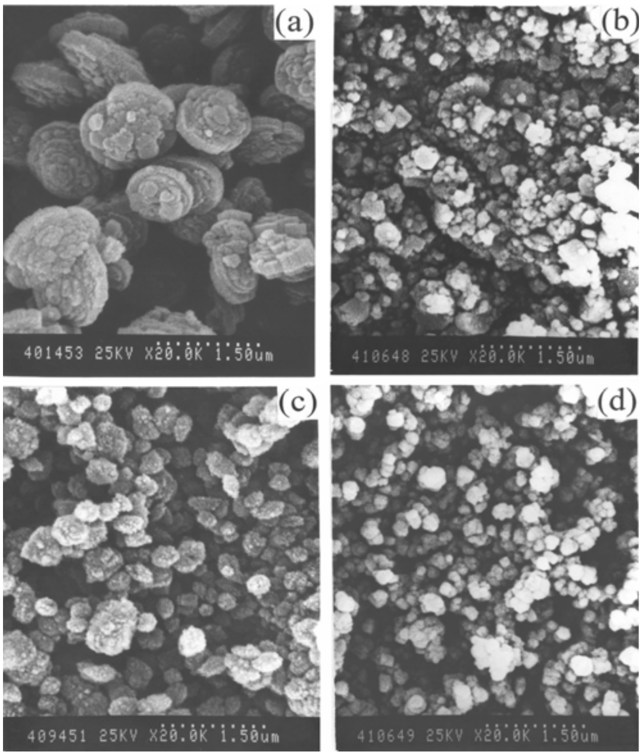

Fig. 9. SEM photographs of zeolite L crystals synthesized from the gel aged for 1 day using Ludox and Zeosil as silica source under static condition at 443 K. (a) Ludox, (b) Ludox (1 day aging), (c) Zeosil, and (d) Zeosil (1 day aging).

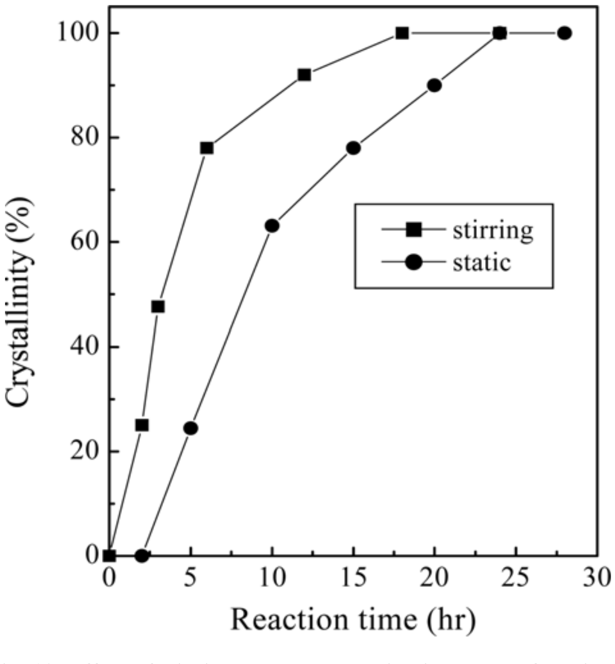

Fig. 10. Effect of stirring on the crystallization rates of zeolite L from the substrate composition of $5.4K_2O$-$5.7Na_2O$-Al_2O_3-$30SiO_2$-$500H_2O$ at 443 K. No aging.

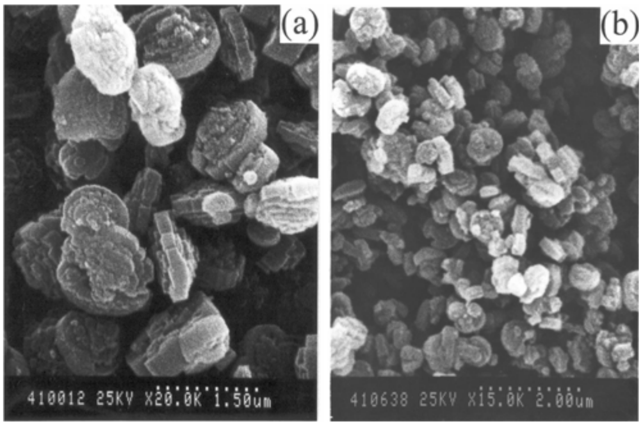

Fig. 11. SEM photographs of zeolite L crystals synthesized under static or stirring at 443 K. (a) under static and (b) under stirring.

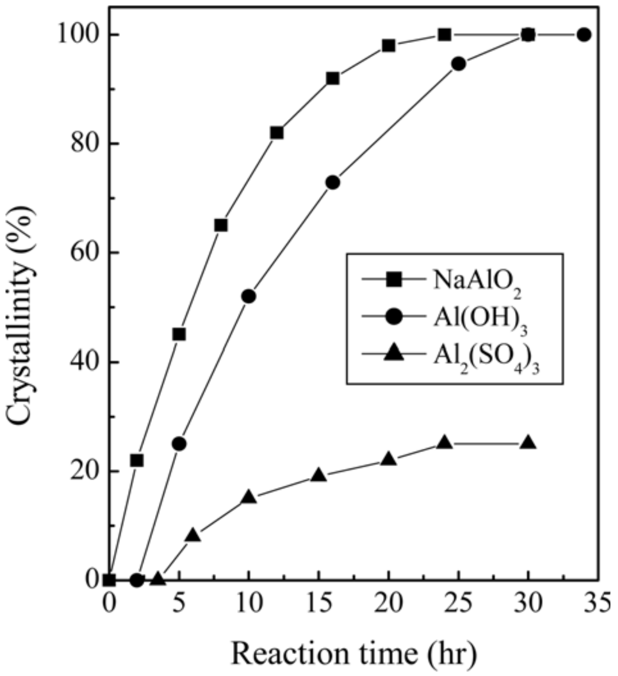

Fig. 12. Effect of different alumina source on the crystallization rates of zeolite L from the substrate composition of $5.4K_2O$-$5.7Na_2O$-Al_2O_3-$30SiO_2$-$500H_2O$ at 443 K. Silica source: Ludox HS-40; no aging.

crystals of about 0.7 μm. Moreover, the crystal habit was very different from those of batches obtained under static condition in the sense that most of the crystals were ice-hockeypuck shaped. When both aging treatment and stirring were used together, the crystal dimension was not smaller than that obtained with stirring alone. This is probably a consequence of the enhanced dissolution of nuclei formed during the aging period upon stirring.

The replacement of sodium aluminate for aluminum hydroxide or aluminum sulfate as alumina source in the synthesis of zeolite L has a great influence on the crystallization of the zeolite L. Fig. 12 shows the effect of different alumina sources on the crystallization rates of zeolite L. The crystallization rate of zeolite L obtained from sodium aluminate as alumina source was observed to be faster than that of the sample prepared with aluminum hydroxide in the gel. When aluminum sulfate was used as alumina source, the degree of crystallization of zeolite L was considerably reduced. No significant differences in crystal size and habit could be observed by SEM among the three samples, indicating that the nature of the alumina source was not as critical as the silica source.

Thermal stability of the zeolite L obtained, which was evaluated by a structural change of the calcined samples at 873-1,273 K for 1 h, was measured by XRD experiment. The X-ray diffraction patterns of the zeolite L obtained with different calcination temperature are shown in Fig. 13(a). It can be seen from the XRD patterns that zeolite L was structurally stable after calcination up to relatively high temperature of 1,173 K and exhibited a change in the crystal structure as revealed by X-ray diffraction patterns after calcination at 1,273 K. The effect of calcination temperature on the degree of crystallinity of zeolite L is shown in Fig. 13(b). Each point on the curves was obtained on a new specimen so that no cumulative effect was observed. The crystallinity of zeolite L started to decrease after calcination at 873 K and decreased sharply with calcination temperature rising from 873-1,273 K.

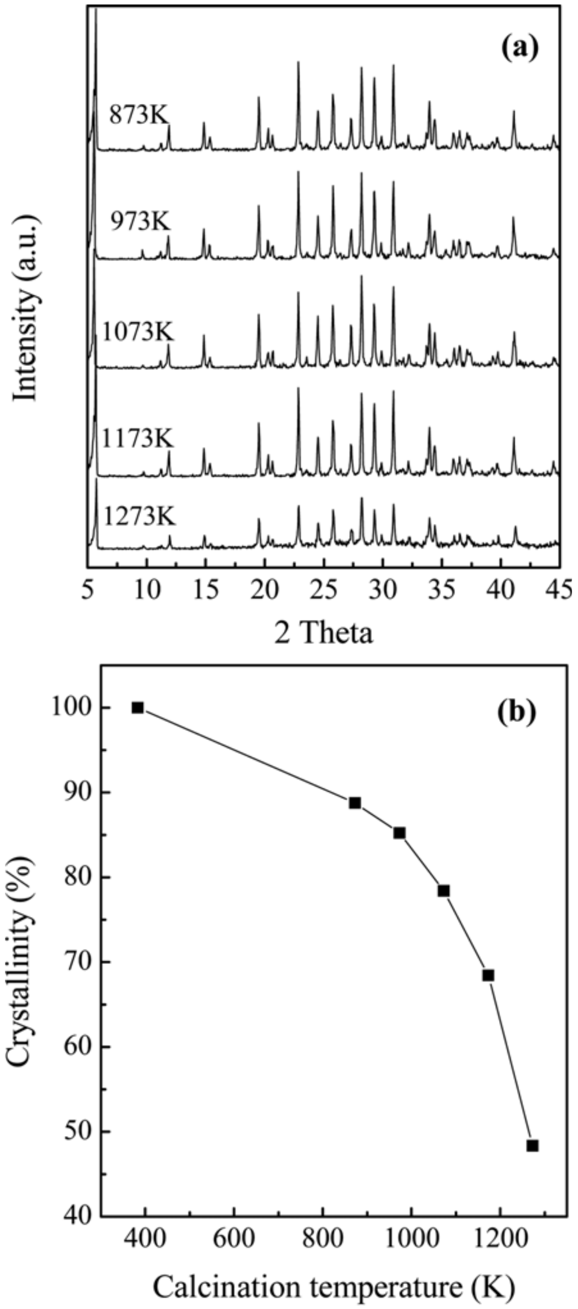

Fig. 13. X-ray diffraction patterns (a) and crystallinity (b) of zeolite L samples at different calcination temperatures.

CONCLUSIONS

A systematic study was carried out to investigate the various factors influencing the synthesis of zeolite L. The concentration of reactants has to be carefully controlled in order to obtain pure zeolite L. In particular, SiO_2/Al_2O_3 ratio must be kept within the range of 25-33 in the synthesis mixture. Critical parameters such as the alkalinity or the water content also greatly influenced the crystallization process of the zeolite L crystals. The crystallizing zeolite structures also depended on the ratio of the cations. There existed the optimum gel compositions of SiO_2/Al_2O_3=30, $(K_2O+Na_2O)/SiO_2$=0.37, $Na_2O/(K_2O+Na_2O)$=0.5 and $H_2O/(K_2O+Na_2O)$=45 for obtaining fully crystalline zeolite L with high yield. Crystallization conditions such as aging of the synthesis gel and stirring also influenced the particle size of zeolite L crystals. Aging treatment at room temperature before hydrothermal treatment of the gel helped in obtaining smaller crystals. Similarly, stirring the gel during crystallization reduced the particle dimensions. The zeolite L synthesized was structurally stable up to 1,073 K; however, the degree of crystallinity of the zeolite L exhibited a substantial decrease at calcination temperatures higher than 873 K.

ACKNOWLEDGMENT

This work was supported by a grant from the Taechon Education & Culture Foundation.

REFERENCES

1. C. Baerlocher, W. M. Meier and D. H. Olson, *Atlas of zeolite framework types*, 5th ed., Elsevier, Amsterdam (2001).
2. A. Corma and H. Garcia, *Eur. J. Inorg. Chem.*, 1143 (2004).
3. S. D. Bhat, P. S. Niphadkar, T. R. Gaydhankar, S. V. Awate, A. A. Belhekar and P. N. Joshi, *Micropor. Mesopor. Mater.*, **76**, 81 (2004).
4. S. D. Bhat, G. M. Chaphekar, P. S. Niphadkar, T. R. Gaydhankar, V. V. Bokade and P. N. Joshi, *Stud. Surf. Sci. Catal.*, **154**, 233 (2004).
5. M. Holzl, S. Mintova and T. Bein, *Stud. Surf. Sci. Catal.*, **158**, 11 (2005).
6. Y. J. Lee, J. S. Lee and K. B. Yoon, *Micropor. Mesopor. Mater.*, **80**, 237 (2005).
7. B. L. Su, V. Norberg, C. Hansenne and A. de Mallmann, *Adsorption*, **6**, 61 (2000).
8. B. L. Su, V. Norberg and C. Hansenne, *Langmuir*, **16**, 1132 (2000).
9. P. N. Joshi, U. D. Joshi, T. H. Kim, K. I. Kim and V. P. Shiralkar, *Adsorption*, **7**, 279 (2001).
10. O. Larlus, L. Tosheva, M. Holzl, S. Mintova, T. Metzger and V. P. Valtchev, *Stud. Surf. Sci. Catal.*, **158**, 367 (2005).
11. T. W. Pechar, S. Kim, B. Vaughan, E. Marand, M. Tsapatsis, H. K. Jeong and C. J. Cornelius, *J. Membr. Sci.*, **277**, 195 (2006).
12. T. W. Pechar, S. Kim, B. Vaughan, E. Marand, V. Baranauskas, J.

Riffle, H. K. Jeong and M. Tsapatsis, *J. Membr. Sci.*, **277**, 210 (2006).
13. S. D. Bhat and T. M. Aminabhavi, *J. Membr. Sci.*, **306**, 173 (2007).
14. A. Arcoya, X. L. Seoane and J. M. Grau, *Appl. Surf. Sci.*, **205**, 206 (2003).
15. J. M. Grau, X. L. Seoane and A. Arcoya, *Catal. Lett.*, **83**, 247 (2002).
16. S. Jongpatiwuta, P. Sackamduang, T. Rirksomboon, S. Osuwan and D. E. Resasco, *J. Catal.*, **218**, 1 (2003).
17. S. Jongpatiwuta, S. Trakarnroek, T. Rirksomboon, S. Osuwan and D. E. Resasco, *Catal. Lett.*, **100**, 7 (2005).
18. S. Nagamatsu, M. Inomata, M. Kishida and K. Wakabayashi, *J. Jpn. Petrol. Inst.*, **44**, 351 (2001).
19. G. Jacobs, W. E. Alvarez and D. E. Resasco, *Appl. Catal. A: Gen.*, **206**, 267 (2001).
20. S. M. Kale and A. P. Singh, *J. Mol. Catal. A: Chem.*, **184**, 399 (2002).
21. W. E. Alvarez and D. E. Resasco, *Catal. Lett.*, **8**, 53 (1991).
22. H. Pan, G. Wei, H. Yuan, Q. Huo, Q. Li, X. Pan, W. Wang and X. Yu, *Stud. Surf. Sci. Catal.*, **170**, 1392 (2007).
23. G. Calzaferri, S. Huber, H. Maas and C. Minkowski, *Angew. Chem. Int. Ed.*, **42**, 3732 (2003).
24. D. Bruhwiler and G. Calzaferri, *C.R. Chimie*, **8**, 391 (2005).
25. C. Minkowski and G. Calzaferri, *Angew. Chem. Int. Ed.*, **44**, 5325 (2005).
26. H. Li, A. Devaux, Z. Popovic, L. D. Cola and G. Calzaferri, *Micropor. Mesopor. Mater.*, **95**, 112 (2006).
27. Y. S. Ko and W. S. Ahn, *Bull. Korean Chem. Soc.*, **20**(2), 173 (1999).
28. Y. S. Ko and W. S. Ahn, *Powder Tech.*, **145**, 10 (2004).
29. P. N. Joshi, A. N. Kotasthane and V. P. Shiralkar, *Zeolites*, **10**, 598 (1990).
30. L. J. Garces, V. D. Makwana, B. Hincapie, A. Sacco and S. L. Suib, *J. Catal.*, **217**, 107 (2003).
31. P. K. Bajpai, M. S. Rao and K. V. G. K. Gokhale, *Ind. Eng. Chem. Prod. Res. Develop.*, **17**, 223 (1978).
32. L. Ghamami and L. B. Sand, *Zeolites*, **3**, 186 (1983).
33. S. Ernst, P. A. Jacobs, J. A. Martens and J. Weitkamp, *Zeolites*, **7**, 458 (1987).
34. P. A. Jacobs and J. A. Martens, *Stud. Surf. Sci. Catal.*, **33**, 58 (1987).
35. R. N. Bhat and R. J. Kumar, *J. Chem. Tech. Biotech.*, **48**, 453 (1990).
36. O. Larlus and V. P. Valtchev, *Chem. Mater.*, **16**, 3381 (2004).
37. S. Mintova and V. Valtchev, *Micropor. Mesopor. Mater.*, **55**, 171 (2002).
38. D. M. Ginter, A. T. Bell and C. J. Radke, *Zeolites*, **12**, 742 (1992).
39. A. A. Brock, G. N. Link, P. S. Poitras and R. W. Thompson, *J. Mater. Chem.*, **3**, 907 (1993).
40. K. E. Hamilton, E. N. Coker, A. Sacco, A. G. Dixon and R. W. Thompson, *Zeolites*, **13**, 645 (1993).
41. K. R. Franklin and B. M. Lowe, *Zeolites*, **8**, 495 (1988).